Meteoritics & Planetary Science 38, Nr 7, 1093–1107 (2003)
Abstract available online at http://meteoritics.org

Impact tectonics in the core of the Vredefort dome, South Africa: Implications for central uplift formation in very large impact structures

C. LANA, R. L. GIBSON, and W. U. REIMOLD*

Impact Cratering Research Group, School of Geosciences, University of the Witwatersrand, Private Bag 3, P.O. Wits 2050, Johannesburg, South Africa
*Corresponding author. E-mail: reimoldw@geosciences.wits.ac.za

(Received 10 September 2002; revision accepted 16 June 2003)

Abstract–The 80 km wide Vredefort dome presents a unique opportunity to investigate the deep levels of the central uplift of a very large impact structure. Exposure of progressively older strata in the collar of the dome and of progressively higher-grade metamorphic rocks toward its center is consistent with differential uplift; however, the deepest levels exposed correspond to pre-impact mid-crust, rather than lower crust, as has been suggested previously. Pre-impact Archean gneissic fabrics in the core of the dome are differentially rotated, with the angle of rotation increasing sharply at a distance of ~16–19 km from the center. The present asymmetric dips of the collar strata, with layering dipping outward at moderate angles in the southeastern sector but being overturned and dipping inward in the northwestern sector, and the eccentric distribution of the pre-impact metamorphic isograds around the core of the dome can be reconciled with symmetric rotation of an initially obliquely NW-dipping target sequence during central uplift formation. The rocks in the core of the dome lack distinctive megablocks or large-slip-magnitude faults such as have been described in other central uplifts. We suggest that the large-scale coherent response of these rocks to the central uplift formation could have been accommodated by small-scale shear and/or rotation along pervasive pseudotachylitic breccia vein-fractures.

INTRODUCTION

That large impact events are capable of promoting intense structural and thermal modification of deep levels of the earth's crust is now widely recognized (e.g., Grieve 1987; Melosh 1989; French 1998; Ivanov and Deutsch 1999). Structural modification is attributed to gravitational collapse of the unstable bowl-shaped transient crater cavity that forms immediately following an impact (Grieve 1987; Melosh 1989). While small craters display only inward slumping of the crater walls, large (complex) craters are characterized by additional extreme vertical uplift in their central parts, which forms a distinctive dome-shaped central uplift. The exact mechanism by which this collapse proceeds is not fully understood; however, the speed with which the uplift and rotation necessary to form central uplifts occurs implies that the strength of the rocks in the subcrater basement is drastically reduced during and immediately after passage of the impact shock wave (Melosh 1989). Melosh (1979) proposed that this temporary strength degradation might be achieved by strong vibrations triggered by the shock wave in the subcrater basement—a process referred to as acoustic fluidization. Ivanov et al. (1996) proposed that these vibrations typically affect fault-bounded blocks between tens and hundreds of meters in size that are, consequently, able to oscillate independently of their neighbors. While most central uplifts display abundant evidence of smaller-scale faulting, the complexity of the stresses involved in their formation (initial centripetal and tangential compressional stresses during uplift, followed by centrifugal motion during late-stage collapse) makes it difficult to corroborate these fluidization models through direct geological observation.

Well-documented deep levels of impact crater basement are extensively exposed in the Vredefort dome, the eroded remnant of the central uplift of the 2.02 Ga Vredefort impact structure (e.g., Grieve and Therriault 2000; Gibson and Reimold 2001 and literature therein). Current estimates for the depth of erosion range between 5 and 10 km (e.g., McCarthy et al. 1986, 1990; Gibson et al. 1998; Henkel and Reimold 1998). The relatively well-exposed section through the structure represents a unique opportunity to investigate structural modifications within the interior of the central uplift of a giant impact structure. In this paper, we present the results of structural mapping of the core of the Vredefort dome that place constraints on the structural development of the Vredefort central uplift.

GEOLOGICAL SETTING

The Vredefort dome is a prominent, ~80 km wide, structural and geophysical feature located ~120 km southwest of Johannesburg, South Africa (Fig. 1). It is surrounded by a 50–70 km wide rim synclinorium, which encompasses much of the gold-rich Witwatersrand basin (Fig. 1a). The dome consists of an ~40 km wide, early Archean crystalline basement core, which is enclosed by a 15–20 km wide collar of late Archean to Paleoproterozoic supracrustal strata (Fig. 1b). These supracrustal rocks, which range in age from 3.07 to ~2.1 Ga (Armstrong et al. 1991), belong to (from the oldest to the youngest) the Dominion Group and the Witwatersrand, Ventersdorp, and Transvaal Supergroups. In the western, eastern, and northern sectors, the collar strata are generally subvertical to overturned, while in the southeastern sector the collar strata dip 30°–40° SE (Fig. 1b). The right-way-up orientation and shallow dips of the supracrustal strata in the southeastern sector are confirmed by borehole data (e.g., Antoine et al. 1990; Brink et al. 1997). The collar rocks show elevated pre-impact metamorphic grades relative to the rest of the Witwatersrand region, with mid-amphibolite facies metamorphism in the Dominion Group and Lower Witwatersrand Supergroup in the inner collar of the dome (e.g., Bisschoff 1982; Gibson and Wallmach 1995). The metamorphic isograds are, however, eccentric with respect to the collar strata, with progressively younger strata affected toward the northwestern collar (Bisschoff 1982; Gibson and Wallmach 1995) (Fig. 1b).

Crystalline basement lithologies in the core of the dome comprise predominantly polydeformed Archean migmatitic gneisses, with subsidiary mafic and metasedimentary xenoliths. These rocks experienced mid-crustal, upper amphibolite- to granulite-facies metamorphism at ~3.1 Ga (e.g., Stepto 1979, 1990; Hart et al. 1999; Moser et al. 2001; Lana et al. 2003, Forthcoming), shortly before the commencement of deposition of the Dominion Group lavas. In

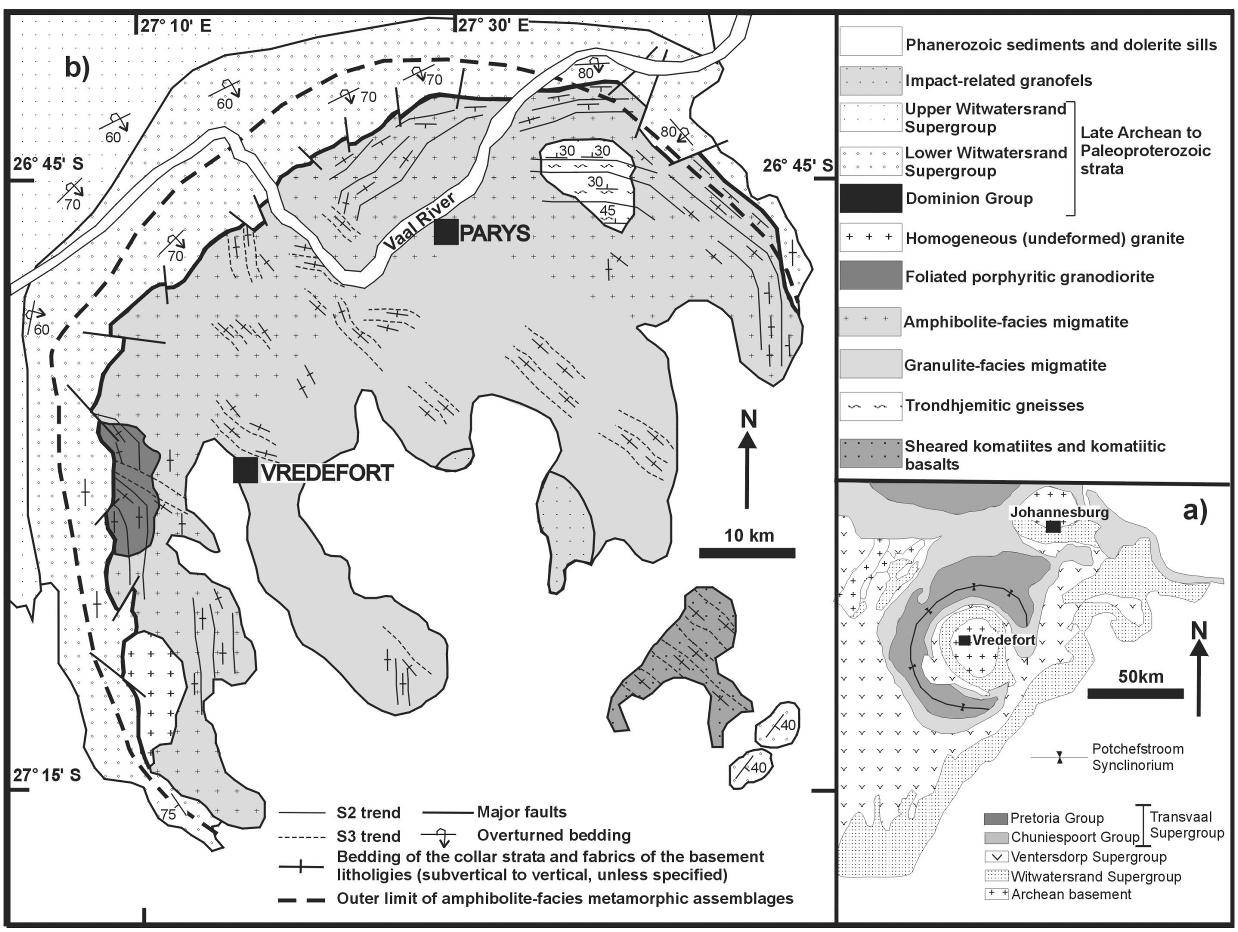

Fig. 1. a) Simplified geological map showing the distribution of Archean and Paleoproterozoic rocks in the Witwatersrand basin and the axis of the Potchefstroom Synclinorium. The southern and southeastern parts of the basin are covered by younger sediments and have been constrained by geophysical methods and boreholes; b) simplified geological map of the Vredefort dome showing the main lithologies and structures in the collar and core of the dome, and the eccentric distribution of the pre-impact metamorphic isograd (discussed in the text).

the southeastern sector, a greenstone sequence of sheared metavolcanics and subordinate mafic-intermediate tuffaceous units is exposed as an inlier within Phanerozoic sediments and dolerite sills of the Karoo Supergroup (Minnitt et al. 1994; Lana et al. 2002) (Fig. 1b). Much of the southeastern part of the dome is obscured beneath these sediments and sills.

The presence of impact-diagnostic features, such as shatter cones, high-pressure quartz polymorphs, and decorated planar deformation features in quartz and zircon, in rocks of the dome leaves no doubt that the dome is the eroded remnant of a giant impact structure (see reviews by Grieve and Therriault 2000; Gibson and Reimold 2001). In addition, outcrops in the dome expose a pervasive network of cm- to m-spaced pseudotachylitic breccia-filled fractures (Reimold and Colliston 1994; Gibson et al. 1997). Large dikes of pseudotachylitic breccia up to tens of meters wide and hundreds of meters long rival the dikes of impact melt rock (the Vredefort Granophyre; Koeberl et al. 1996) in size. A 2.02 Ga age for the Vredefort Granophyre and pseudotachylitic breccia (Spray et al. 1995; Kamo et al. 1996) is now widely accepted as the age for the Vredefort impact event.

The rocks in the dome are variably affected by an impact-induced thermal metamorphic overprint, which increases in grade radially inward from ~300°C in the collar rocks to >1000°C in the center of the dome (Gibson et al. 1998, 2002; Gibson 2002). Estimates from geobarometry on the post-impact metamorphic assemblages indicate that between 7 and 10 km of overburden has been removed since the impact event (Gibson et al. 1998). These estimates are consistent with results of geophysical modeling of the impact structure (Henkel and Reimold 1998) and regional stratigraphic correlations (McCarthy et al. 1990), and they explain the absence of an impact melt sheet and crater fill breccias that are still observed in other large complex craters such as Sudbury and Chicxulub (e.g., Grieve and Therriault 2000). This great depth of erosion poses problems for estimates of the original crater dimensions. Most estimates for the crater diameter range between 250 and 300 km (Henkel and Reimold 1998; Grieve and Therriault 2000), although Turtle and Pierazzo (1998) suggested a significantly smaller crater diameter of between 150 and 200 km, based on numerical modeling.

LITHOLOGIES AND ARCHEAN DEFORMATION IN THE CORE OF THE VREDEFORT DOME

The lithologies in the exposed northern half of the basement core of the Vredefort dome are migmatites and gneisses produced during partial melting and deformation of the early Archean tonalite-trondhjemite-granodiorite-greenstone crust at mid-crustal levels at 3.1 Ga (Stevens et al. 1997; Hart et al. 1999; Lana et al. 2003, Forthcoming). The migmatites are melt-rich with granitic leucosome bands alternating with trondhjemitic and tonalitic melanosome bands. Locally, the migmatites are intruded by syn-tectonic porphyritic granodiorites and undeformed homogeneous granites (Fig. 1b). The gneisses within 4–5 km of the center of the dome display extensive impact-related recrystallization (granofels zone, Fig. 1b; Gibson et al. 2002).

The basement rocks record fabrics that developed during at least 4 Archean deformation events (Lana et al. 2001, 2002, 2003, Forthcoming) (Fig. 2). The earliest fabric (here referred to as S1) is defined by a gneissic foliation, which is locally accentuated by foliation-parallel plagioclase-quartz veins (Fig. 3a). S1 is, however, largely transposed by S2 and S3 fabrics, which are defined by amphibolite- to granulite-facies migmatitic layering (Figs. 3b and 3c). Close to the collar-basement unconformity, S2 is subvertical and has a tangential strike parallel to the strike of the collar rocks (Fig. 2, insets 1–3, 5, 6, 8–11; Fig. 4a). At distances of more than 3–6 km from this contact, S2 dips moderately steeply at 30° to 40° north, although the strike remains tangential (Fig. 2, insets 7 and 9). In the central parts and northwestern and southwestern sectors of the dome, S2 is transposed by NW-trending, vertical, and D3 high-strain zones (Fig. 2, insets 1–4, 6, 7, 12–15). The S2 fabric is deformed into open to tight, upright, and shallow to moderately NW- or SE-plunging folds (Figs. 3c, 4a). In low-strain lenses in these areas, S2 is subhorizontal (Fig. 2, insets 13–15).

Although mineral stretching lineations are conspicuously absent in the stromatic migmatitic bands, metapelites and mafic granulites located some 5–7 km northwest from the center show oriented crystals of biotite and pyroxene, which define a peak-metamorphic L3 lineation (Fig. 4a; inset for the central parts). L3 plunges dominantly at 20°–40° NW, but in areas of intense D3 folding, it may change orientation from NW to N and SE (Fig. 4a). These local-scale variations in L3 orientation and the D3 double-plunging folds, which are prominent features in the central areas of the dome (Fig. 4a), might indicate pre-impact periclinal folding of the S2 fabric. In the mafic-ultramafic schists (sheared metavolcanics) of the Greenlands Greenstone Complex (southeastern sector of the dome), L3 plunges dominantly at 30°–40° SE (Fig. 4a). This significant change in L3 orientation, from NW-plunging in the central parts to SE-plunging in the southeastern sector, is attributed to rotation linked to the doming event (discussed below).

The S4 fabric occurs in a mylonitic shear zone (termed the Broodkop Shear Zone by Colliston and Reimold [1990]) that separates the metavolcanics of the Greenlands Greenstone Complex and the migmatitic gneisses in the northern and central parts of the dome (Colliston and Reimold 1990; Lana et al. 2002). This shear zone is characterized by high-temperature retrograde mineral assemblages that indicate a late-metamorphic timing for D4. The truncation of S3 and S4 features by the collar-basement unconformity indicates a >3.07 Ga (Dominion Group; Armstrong et al. 1991) age for these tectonic events. All the above fabrics are crosscut by pseudotachylitic breccia.

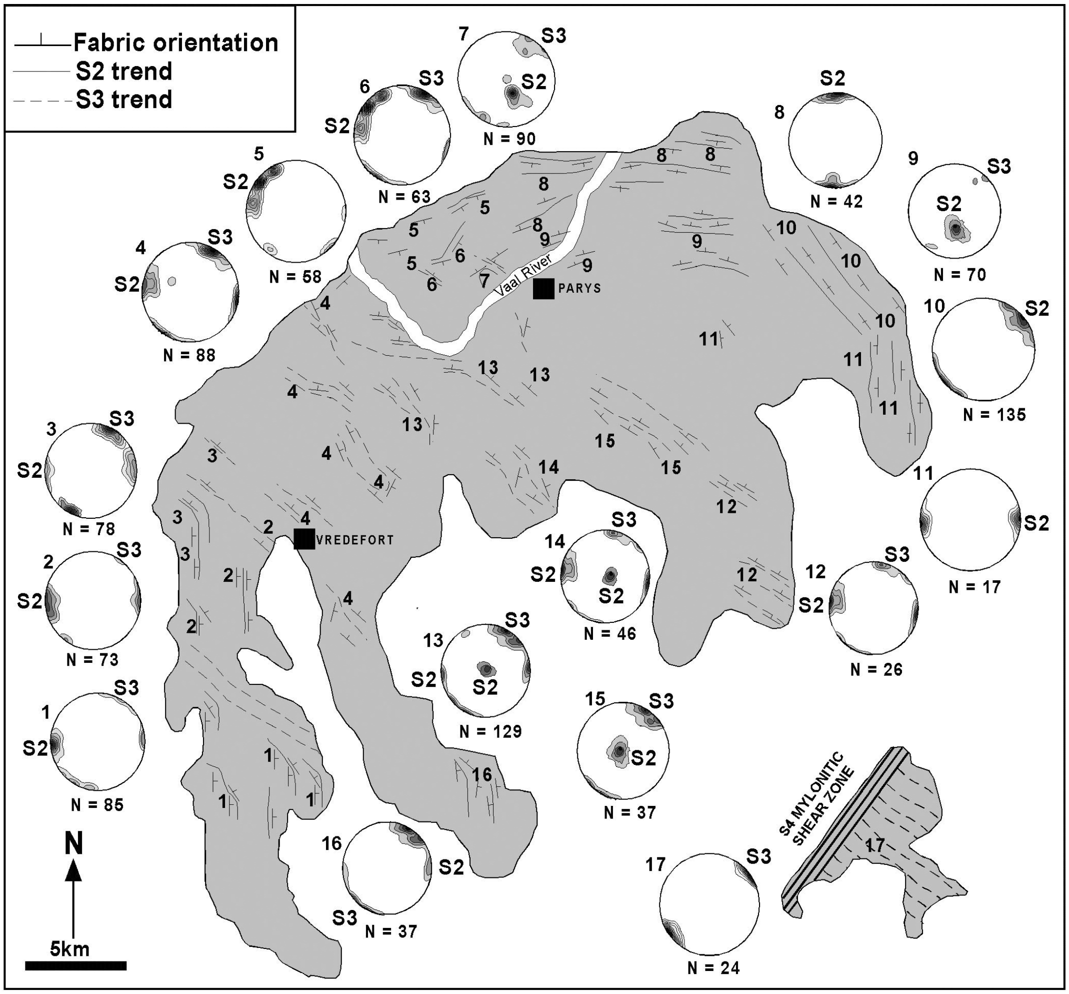

Fig. 2. Simplified structural map of the basement core of the Vredefort dome showing structural contours and orientation data for the S2 and S3 fabrics and the location of the mylonitic Broodkop shear zone (S4). Equal-area, lower hemisphere contoured stereonets show poles to the S2 and S3 fabrics measured at 17 localities.

DEFORMATION RELATED TO THE IMPACT EVENT

Pseudotachylitic Breccia

The most ubiquitous, mesoscopic, impact-related feature in the dome is pseudotachylitic breccia, which occurs in mm- to m-wide pods and veins within pervasive vein-fracture networks in almost all rocks in the dome. More rarely, the breccia occurs in dikes, the largest of which exceed several hundred meters in length and tens of meters in width. These dikes are principally seen in the outer parts of the core of the dome (Reimold and Colliston 1994). Pseudotachylitic breccias are also seen in the granofels zone in the center of the structure, but they are volumetrically minor compared with the dikes in the outer core and are strongly overprinted by high-temperature thermal effects triggered by shock heating (Gibson et al. 2002).

Martini (1991) described coesite ± stishovite associated with melt breccia veins from 17 localities in the collar of the dome and concluded that the veins formed under shock conditions. He proposed that the extreme localization of elevated shock pressures was achieved primarily by the collapse of voids (pre-existing joints) and that melting was assisted by frictional heating caused by differential acceleration of layers along microfaults. According to Martini (1991), however, the bulk of the pseudotachylitic breccia veins in the dome lack shock-diagnostic features. He concluded that these breccias formed by post-shock frictional melting during central uplift rebound. Reimold et al. (1992), however, expressed concern with this somewhat arbitrary subdivision of pseudotachylitic breccias based on an unspecified limiting volume of melt. Recent observations, including structural continuity between thin and thick veins and evidence of enhanced shock effects along the margins of both thick and thin veins, suggest that many more, if not the bulk, of the pseudotachylitic breccias in the dome formed during shock compression, with or without a frictional heating component (Gibson et al. 2002; Gibson and Reimold 2003). In

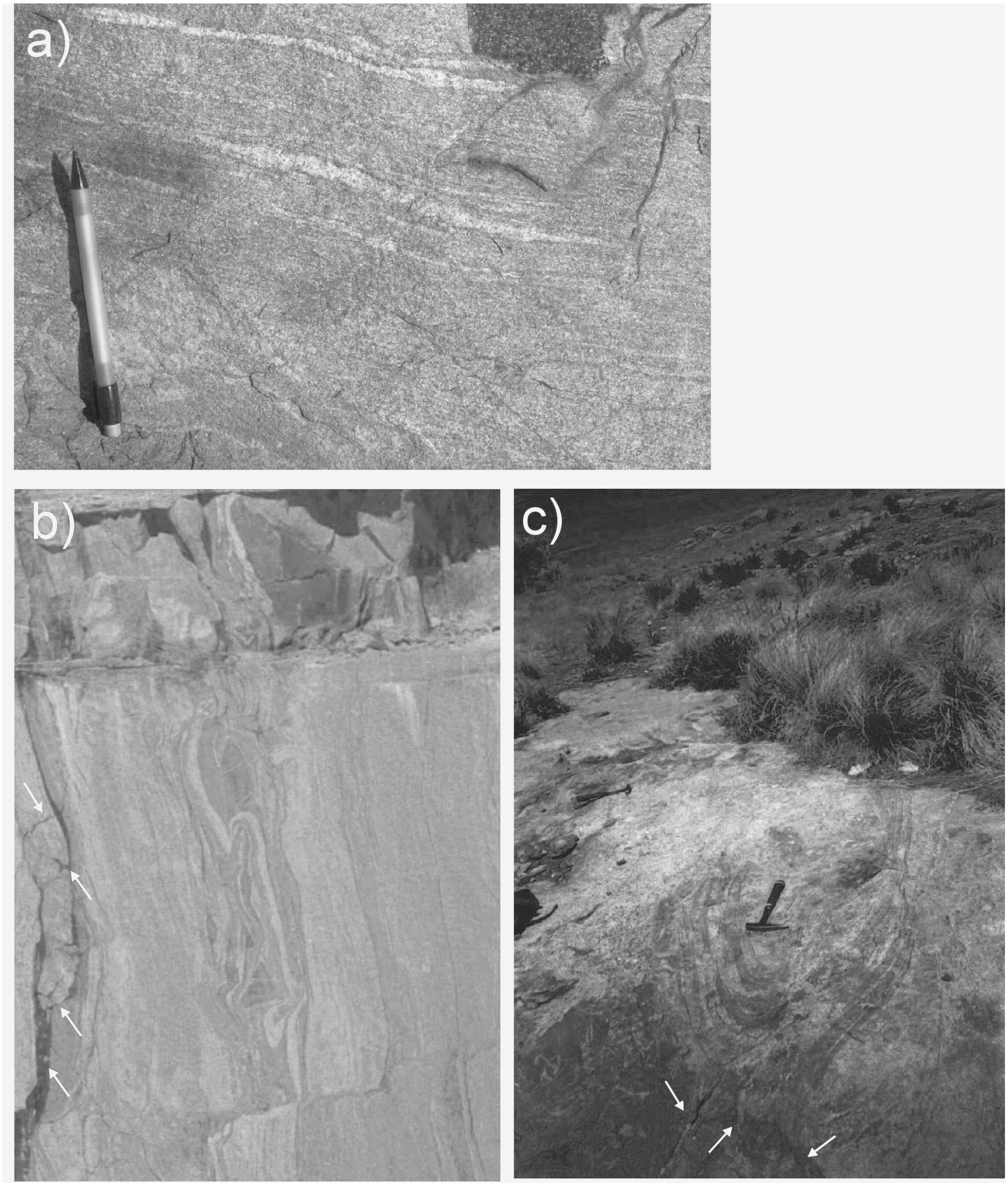

Fig. 3. a) Trondhjemitic gneiss with S1 foliation. Otavi quarry, northeast of Parys; b) Migmatite with subvertical S2 foliation. Boudins of trondhjemitic gneiss (dark grey) lie in a banded granitic-trondhjemitic gneiss matrix. Leeukop quarry, north of Parys; c) folded S2 foliation in subvertical S3 high-strain zone in trondhjemitic gneiss. The fold plunges shallowly to the NW and is disrupted by granitic leucosome that displays a weak S3 fabric. The locality is 4 km SW of Parys. The black vein networks (white arrows) in (b) and (c) are impact-related pseudotachylitic breccia.

this model, melts that did not quench immediately were mobilized along the fracture network during the compression and modification stages of the impact event, ultimately ponding in extensional sites. The latter may explain how the voluminous dikes of pseudotachylitic breccia with exotic clasts that must have traveled at least tens of meters (Reimold and Colliston 1994) could form without any evidence of large displacements along their margins or in the surrounding rocks.

No fault zones with large slip magnitudes are observed in the core of the dome, although displacements of up to

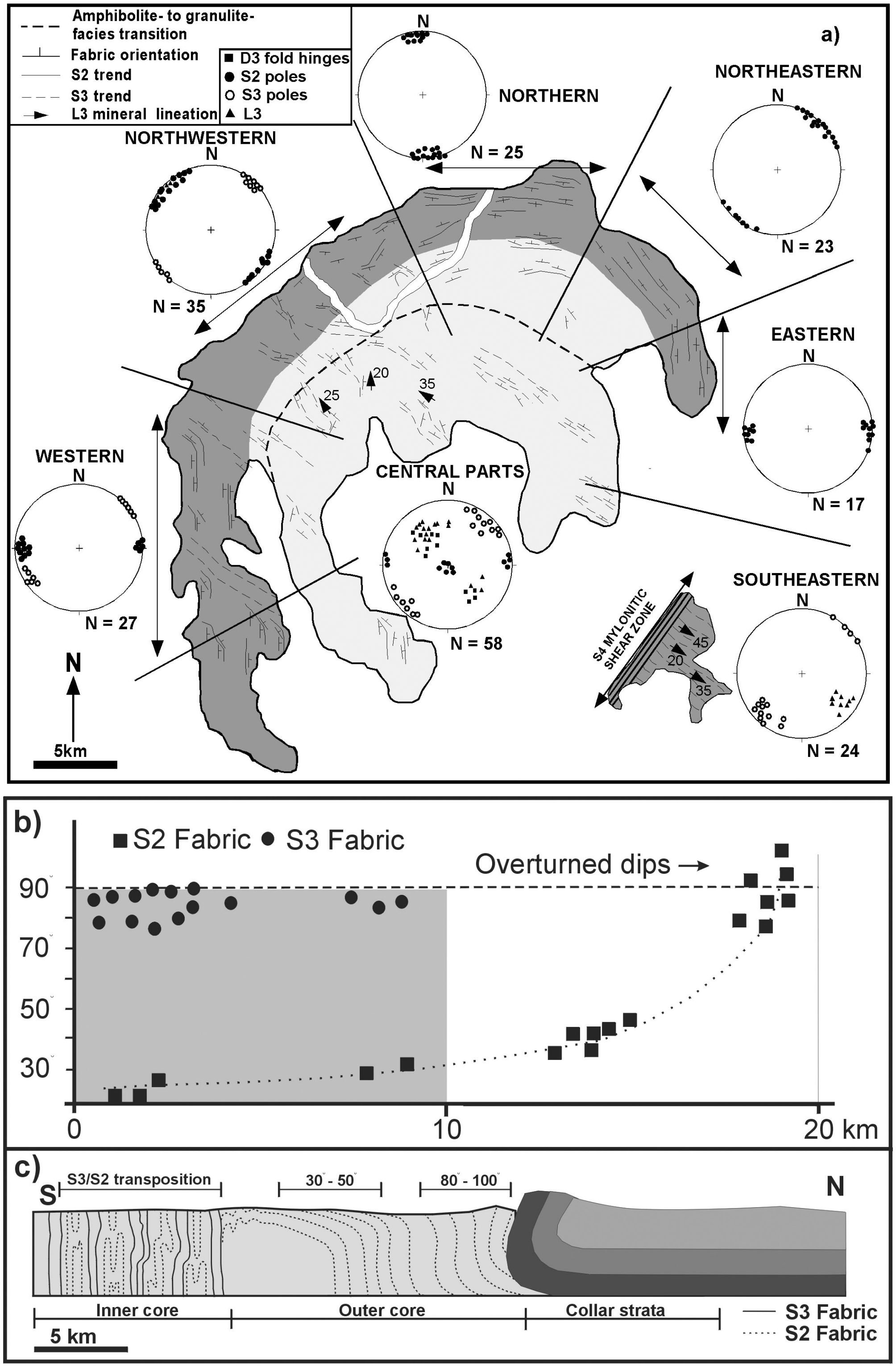

Fig. 4. a) Simplified structural map of the core of the Vredefort dome showing the 6 sectors used in the rotation analysis. The arrows indicate trends of rotation axes parallel to the strikes of bedding in the collar strata. Equal-area, lower hemisphere stereonets show the reduced data sets used in the rotations. The dark gray shade indicates zones of strong rotation of the basement fabrics; b) schematic dip angle versus distance diagram showing the increase in rotation of the S2 fabric with increasing radial distance in the northern sector of the dome. The gray shaded area indicates the extent of S2/S3 transposition in the central parts of the dome; c) schematic N-S cross-section showing an interpretation of the structural data set, with transposition of S2 into S3 in the inner core, increasing rotation of S2 in the outer core, and overturned collar strata.

hundreds of meters have been established along radial faults in the collar rocks (Wieland et al. 2003). While this may, at least in part, reflect the diminished levels of exposure of the core rocks, that small displacements along the pseudotachylitic breccia veins are commonplace is worth noting. The maximum measured displacement along a pseudotachylitic breccia vein in the Vredefort dome is ~1 m (Reimold and Colliston 1994) but, in most cases, the migmatitic and gneissic banding shows no signs of significant (i.e., greater than a few mm to cm) vein-parallel displacement and no sharp fabric rotation. These small displacements may reflect reactivation of the melt-lubricated, shock-induced fabric network during crater collapse.

Voluminous fault-related pseudotachylitic breccias associated with the impact event are, however, known from the gold fields in the Witwatersrand basin on the outer limb of the Potchefstroom synclinorium west of Johannesburg (Fig. 1a). Killick (1993) has shown that these breccias formed during extensional slip along shallow faults dipping toward the dome. The ~2.01–2.02 Ga ^{40}Ar-^{39}Ar age obtained by Trieloff et al. (1994) for some of these breccias confirms their genesis during the impact event. Their geometry suggests that they are linked to the inward slumping of the transient cavity walls during the crater modification phase. Although zones of pseudotachylitic breccia up to 30 m wide have been noted along these faults, km-scale breccias reminiscent of those believed by Spray (1997) to indicate collapse-related "superfaults" in the Sudbury structure have not been found.

Rotation of Fabrics in the Outer Parts of the Basement Core

Seismic sections across (Brink et al. 1997; Friese et al. 1995), and geophysical modeling of (Henkel and Reimold 1998), the Vredefort impact structure indicate a minimum of 9 km of uplift of the unconformity between the Archean basement gneisses and supracrustal rocks during the Vredefort event. Given that estimates of post-impact erosion range between 5 and 10 km and that the collar strata represent an ~11 km thick supracrustal pile, the total amount of uplift may well have exceeded 15 km. The subvertical to overturned orientation of bedding in the collar rocks around most of the dome (Fig. 1b) testifies to strong rotation associated with formation of the central uplift.

In the outer parts of the core of the dome, differentiated mafic sills that must have cooled in a horizontal orientation (Bisschoff 1973) currently display a vertical orientation, indicating that the upturning visible in the collar rocks extends at least a short distance into the core of the dome. The strong rotation of the S2 fabric, from subhorizontal in the center of the dome to subvertical-tangential in the outer 3–6 km of gneiss exposure (Fig. 2, insets 8–11; Fig. 4), supports this and constrains the extent of strong doming-related rotation. This transition is observed in the northern and eastern parts of the dome (Figs. 4b and 4c), but the amount of rotation in the northwestern sector is not clearly seen because of the presence of the vertical NW-trending S3 fabric.

ROTATION ANALYSIS

The collar rocks dip asymmetrically around the dome with strong overturning in the northwestern sector opposed by moderate normal dips in the southeastern sector (Fig. 1b). In the eastern and western sectors, average dips are subvertical to slightly overturned (Bisschoff 2000). Geophysical surveys and exploration boreholes drilled in the southeastern sector of the dome beneath the Karoo Supergroup cover (e.g., Brink et al. 1997) also indicate that the upper parts of the ~11 km thick supracrustal sequence exposed in the northern collar are largely missing (Fig. 1a). Three possible explanations exist for this asymmetry: 1) post-impact tilting of an originally symmetric central uplift structure; 2) asymmetric rotation of originally flat-lying supracrustal strata during central uplift formation; or 3) symmetric rotation of originally inclined supracrustal strata.

Regional geological compilations (McCarthy et al. 1990; Friese et al. 1995) have suggested that post-impact tilting could have caused the asymmetric orientation of the collar strata in the Vredefort dome. Although McCarthy et al. (1990) do not explicitly state the age of the tilting, Friese et al. (1995) suggested that NW-directed thrusting and tilting in the Witwatersrand basin could be linked to the circa 1100 Ma Namaqua-Natal orogenic event along the southern margin of the Kaapvaal craton. In both cases, the angle of tilt is small—only 3° in the case of McCarthy et al. (1990)—and insufficient to account for the variable dips in the collar strata; neither does it explain the eccentric isograd distribution in the collar rocks. We, thus, attempt to evaluate the other 2 possible explanations by reconstructing the pre-impact orientations of the collar strata and basement fabrics.

To evaluate these 2 scenarios, we consider the dome as a polygonal structure with 6 sectors (or structural domains) in which the basement fabrics and collar strata were rotated about an axis parallel to the present strike of the strata (Fig. 4a). In the first scenario, rotation angles are based on the assumption that the collar strata were subhorizontal before impact and, thus, that they must have rotated by different amounts in each sector (asymmetric rotation). In the second scenario, this prerequisite is absent and the strata are rotated by the same amount in each sector (symmetric rotation).

Note that these scenarios represent first-order approximations aimed at understanding a very complex process (as can be seen from the complex bedding and fabric orientations both between and within the polygon segments; Bisschoff 2000; Wieland et al. 2003). To avoid these complexities and the complexity caused by the D3 folding and shearing of the S2 foliation, only measurements that represent the general fabric and bedding orientations in each sector have been selected for rotation.

Asymmetric Rotation

To evaluate the patterns produced by asymmetric rotations around the dome, the fabric and bedding data were back-rotated by a range of angles from 90° to 120° in the northern half of the dome and by 30° to 50° in the southeastern sector. These ranges cover the spectrum of bedding dip angles found in individual sectors. Fig. 5 presents the rotations for which the most consistent pre-impact S2 orientations were achieved. These results were obtained when the collar strata were rotated by between 90° and 110° in the northern, western, eastern, and northeastern sectors, and by 40° in the southeastern sector (Fig. 1b). The angles and axes of rotation are presented together with the main results of back-rotation in Fig. 5. The mean values of the rotated S2 and S3 fabrics are presented in Table 1.

In the eastern, northeastern, northern, and western sectors, the asymmetric back-rotation produces a subhorizontal to shallowly SW-dipping pre-impact orientation for S2 (Figs. 5a–5c and 5e; Table 1). In the northwestern and southeastern sectors, however, back-rotation does not change the S3 orientation, which remains subvertical NW-trending, while S2 in the northwestern sector is restored to a shallow SE to E dip (Figs. 5d and 5f; Table 1). Back-rotation of the L3 mineral lineation in the southeastern sector produces a subhorizontal to shallowly NW-plunging pre-impact orientation (Fig. 5f). Back-rotation of fabrics in the western sector produces a moderately steeply S-dipping S3 orientation (Fig. 5e), which contrasts with the S3 orientation in the rest of the dome core. A subvertical NW-trending orientation for the S3 fabric in this sector is only obtained when S3 is rotated about axes oriented 020° to 030°, which cannot be justified from the present strike of bedding.

Symmetric Rotation

To evaluate the patterns produced by symmetric rotations during central uplift formation, the fabric and bedding data of each sector were uniformly back-rotated. As with the first scenario, we used angles of rotation ranging from 70° to 120°, but the best clustering of the data was obtained when fabric and bedding were rotated by 90° (Figs. 6 and 7; mean values in Table 1).

Symmetric back-rotation by 90° of the present average

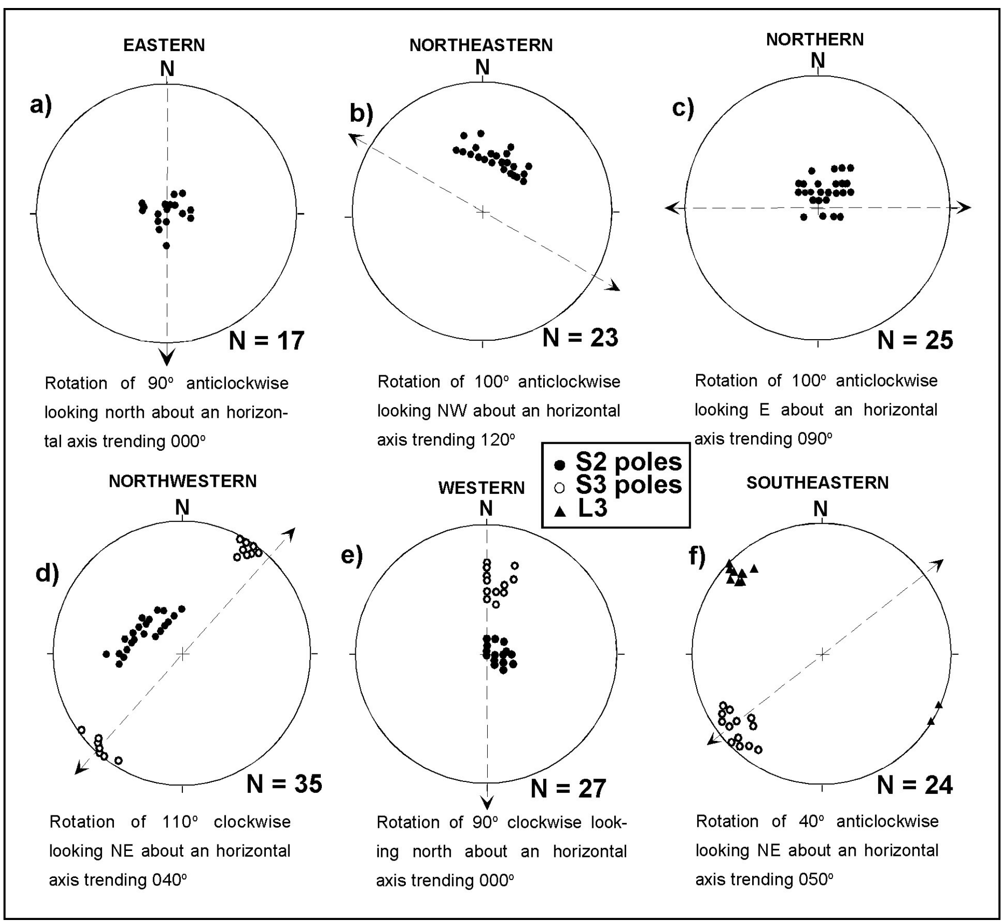

Fig. 5. Back-rotation of poles to the S2 and S3 fabrics in the a) eastern, b) northeastern c) northern, d) northwestern, e) western, and f) southeastern sectors. Restoration assuming horizontal pre-impact orientation of supracrustal strata in each sector.

Table 1. Mean values of dip and dip direction (in degrees) of the basement fabrics and bedding of the collar strata in the Vredefort dome.

		Present orientation		Orientation after back-rotation		Orientation after back-rotation	
				Asymmetric rotation		Symmetric rotation	
Basement fabrics	Sector	Dip direction	Dip angle	Dip direction	Dip angle	Dip direction	Dip angle
S2	Eastern	087	87	269	15	359	1
S2	Northeastern	226	85[a]	198	35	206	4
S2	Northern	180	88	182	5	263	6
S2	Northwestern	126	83[a]	186	43	101	8
S2	Western	091	88[a]	162	9	309	8
S3	Northwestern	217	87	071	78	047	82
S3	Western	042	89[a]	181	60	182	40
S3	Southeastern	044	84	041	80	049	83

		Present orientation		Orientation after back-rotation	
				Symmetric rotation	
Collar rocks	Sector	Dip direction	Dip angle	Dip direction	Dip angle
Bedding plane	Eastern	270	90	000	0
Bedding plane	Northeastern	225	80[a]	332	18
Bedding plane	Northern	180	80[a]	000	10
Bedding plane	Northwestern	135	70[a]	322	21
Bedding plane	Western	090	90	000	0
Bedding plane	Southeastern	135	40	330	50

[a]overturned dips.

bedding orientations for the collar strata (Fig. 6b) produces a non-horizontal average pre-impact bedding orientation that is somewhat scattered but which shows a fairly good clustering of poles, indicating a moderate northwesterly dip (Fig. 6c; Table 1).

Back-rotation of the fabrics in the basement lithologies produces a much more consistent, subhorizontal, pre-impact S2 orientation than the asymmetric back-rotation scenario (Figs. 7a–7e). This is particularly seen in the northeastern and northwestern sectors. The mean values of the dip angles for S2 range from 1° to 8°, while mean values for the asymmetric rotation scenario range from 5° to 43° (Table 1). Back-rotation of S3 in the northwestern and southeastern sectors, unsurprisingly, produces a consistent vertical NW trend for the pre-impact orientation, as S3 is perpendicular to the axes of rotation (Figs. 7d and 7f). Back-rotation of S3 in the western sector once again produces an anomalous moderately steeply S-dipping pre-impact orientation (Fig. 7e). Back-rotation of L3 in the southeastern sector produces a moderately steeply NW-plunging pre-impact mineral lineation orientation (Fig. 7e), which is consistent with the orientation of L3 in the central parts of the dome (Fig. 4a).

DISCUSSION

Modification of the Archean Crust During the Uplift Event

The subvertical disposition of the strata in the collar of the Vredefort dome and the increase in metamorphic grade from upper amphibolite- to granulite-facies in the Archean basement core are both consistent with progressively deeper crustal levels being exposed toward the center of the Vredefort central uplift (e.g., Slawson 1976; Hart et al. 1981; Hart et al. 1990a, b). Estimates of the total thickness of crust exposed in the dome range from ~25 km (Hart et al. 1981) to ~36 km (Hart et al. 1990a, b; Tredoux et al. 1999), with the latter authors proposing that upper mantle rocks are also exposed in the center. These values are broadly consistent with the amount of structural uplift predicted for a 250–350 km diameter impact crater based on scaling relations (S.U. = $0.06D^{1.1}$ [Grieve 1981] or S.U. = $0.086\ D^{1.03}$ [Grieve and Pilkington 1996]). The upper estimates of the thickness of crust exposed in the Vredefort dome are, however, problematic from a geometric perspective; for a dome with a radius of only 35–40 km, the only way to expose a 36 km thick crustal profile is if the rocks display a subvertical orientation virtually throughout the radial section. Hart et al. (1990a) found that this "crust-on-edge" geometry required the presence of a major structural discontinuity in the core of the dome. They proposed the existence of a NE-trending crustal-scale shear zone, which they named the Southeast Boundary Fault.

Our results, which represent the first comprehensive structural analysis of the entire crystalline core of the Vredefort dome, not only fail to show any evidence of the central, NE-trending, crustal-scale shear zone proposed by Hart et al. (1990a) (Fig. 1), they also indicate that the amount of impact-related rotation decreases toward the center of the dome. Specifically, they show that the S2 fabric in the outer 3–6 km of the core of the dome is rotated by 90° relative to the

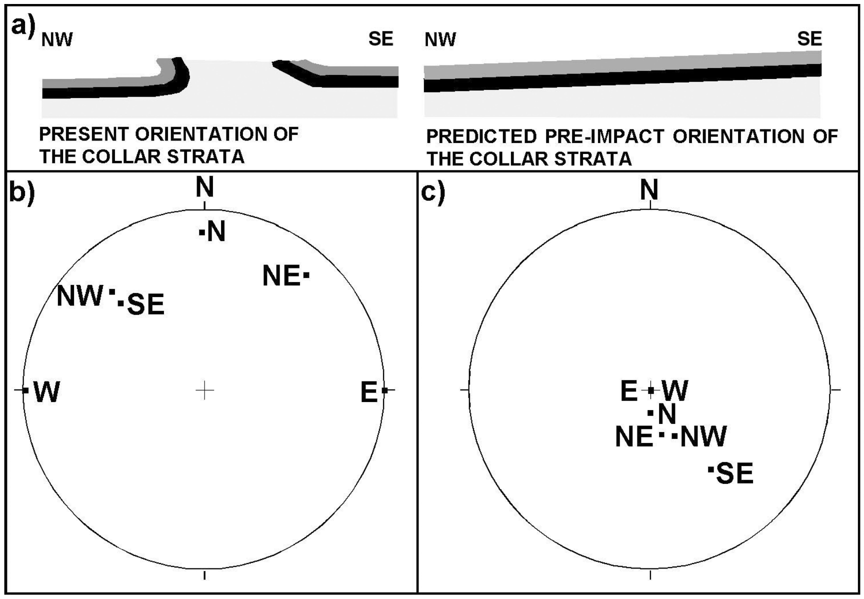

Fig. 6. a) Schematic NW-SE cross-section through the Vredefort dome showing the present and pre-impact orientations of the collar strata for a symmetric 90° rotation. The restoration considers an ideal 90° rotation during the formation of the central uplift; b) average poles to the collar strata in their present attitude measured in the 6 sectors of the dome; c) poles to bedding of the supracrustal strata after 90° back-rotation around bedding strike in each sector. Note that most of the back-rotated poles indicate a moderate northwesterly tilt for the pre-impact orientation of the supracrustal strata.

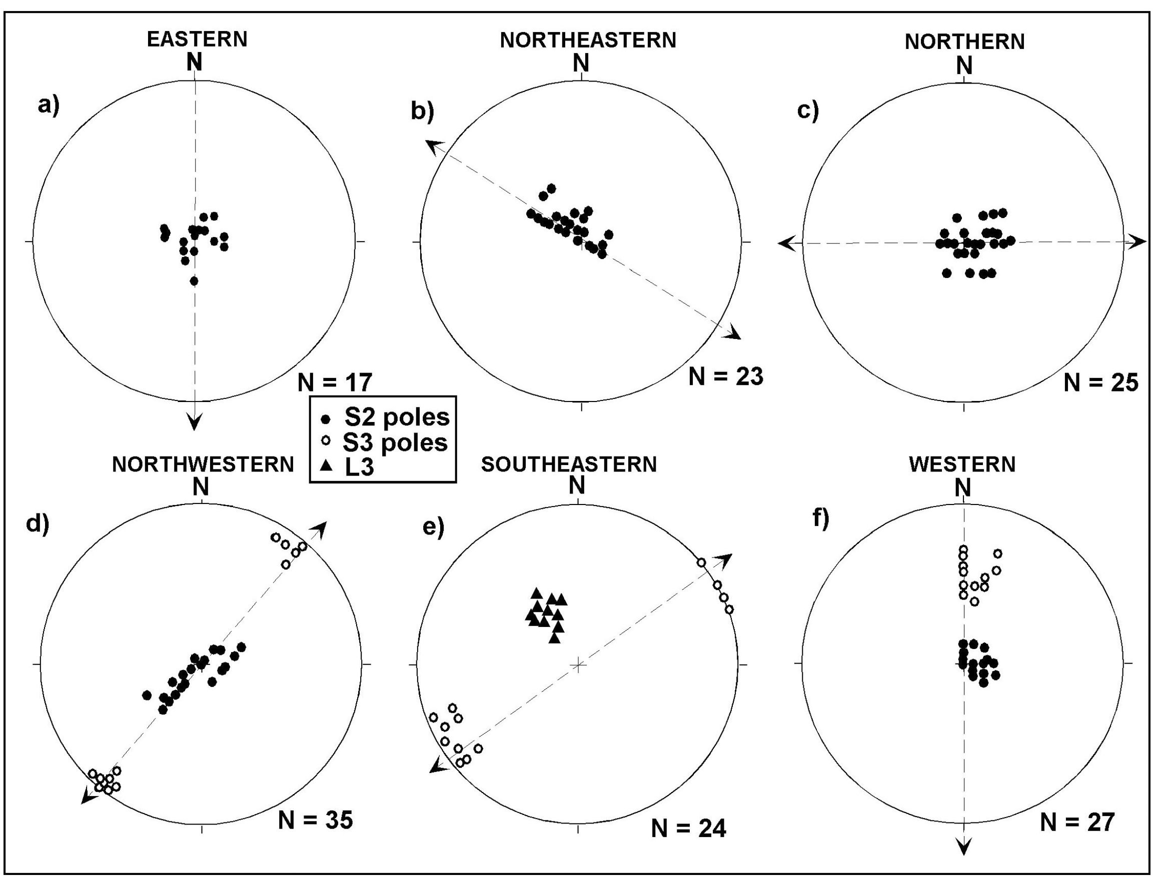

Fig. 7. Back-rotation of poles to the S2 and S3 fabrics in the a) eastern, b) northeastern, c) northern, d) northwestern, e) southeastern, and f) western sectors of the Vredefort dome, assuming uniform 90° rotation about the strike of the supracrustal strata in each sector.

S2 fabric found within a 12 km radius of the center. The transition between the central domain of subhorizontal S2 and the outer domain of subvertical, tangential S2 is comparatively abrupt (Fig. 4c). Overall, S2 describes a mushroom shape rather than a cuspate geometry. This geometry precludes a full 36 km thick crustal section being exposed in the dome. Geobarometric estimates from metamorphic assemblages (Stevens et al. 1997) and lithological mapping and geochemical analysis of the rocks in the core of the dome (Lana et al. Forthcoming) suggest that the deepest levels exposed in the dome correspond to mid-crust rather than lower crust or upper mantle. A similar conclusion was reached by Henkel and Reimold (1998), who proposed maximum uplift of 20–25 km in the core of the Vredefort dome from geophysical modeling of the Vredefort impact structure.

Symmetric Versus Asymmetric Rotation During Central Uplift Formation

The asymmetric orientation of the supracrustal strata in the collar of the Vredefort dome has previously been used to suggest that the dome was the product of an oblique impact directed from southeast to northwest (e.g., Schultz 1997). Numerical modeling of large oblique impacts has shown, however, that the energy distribution within the target rocks is symmetric and, as a consequence, oblique impacts produce symmetric central uplifts (e.g., Ivanov and Artemieva 2002). In the absence of an adequate mechanism to generate >30° tilting of the impact structure after its formation to account for the variable dips in the collar strata, the only remaining explanation for the asymmetry of the dome is that the target stratigraphy was inclined before the impact event. Evidence of Neo-Archean to Paleoproterozoic tectonism that could have generated large-scale tilting of the supracrustal sequence is widespread in the Witwatersrand region (e.g., Roering et al. 1990) and is manifested in the Vredefort dome by km-scale folds in the collar strata as well as thinning and displacement of stratigraphic units across major faults (Martini 1991; Colliston et al. 1999). Based on the evidence presented in Figs. 6 and 7, we conclude that the present asymmetry is most consistent with the formation of a symmetric central uplift in a moderately northwest-dipping target stratigraphy overlying a crystalline basement with a subhorizontal S2 foliation and subvertical NW-trending S3 foliation.

The above model is supported by the eccentric distribution of the pre-impact metamorphic isograds in the dome (Figs. 1b and 8). Although Bisschoff (1982) suggested that the eccentricity indicated the presence of a large subsurface pluton beneath the northwestern sector of the dome, geophysical data (Friese et al. 1995; Henkel and Reimold 1998) provide no support for such a body. Thermobarometric and P-T path constraints from the mid-amphibolite facies assemblages in the Witwatersrand Supergroup rocks in the dome led Gibson and Wallmach (1995) to propose that the metamorphism reflects heating of the Kaapvaal crust by a massive influx of mafic to ultramafic magmas during the 2.06 Ga Bushveld magmatic event. This is supported by $^{40}Ar/^{39}Ar$ dating of the metamorphic assemblages (Gibson et al. 2000). The immense scale of the Bushveld magmatothermal event suggests that the metamorphic isograds would have formed with an original horizontal attitude through large parts of the craton. Given that only 40 Ma separate the Bushveld and Vredefort events, the likelihood that isograds were still subhorizontal at the time of the impact is high. Thus, the fact that the isograds cut downward through the supracrustal stratigraphy in the collar of the dome toward the south and east is consistent with the supracrustal rocks having already been tilted down to the northwest at the time of this (pre-impact) metamorphism (Fig. 8).

A regional northwest tilt of the target stratigraphy does not explain all the structural complexity in the Vredefort dome. Apart from the large folds and faults mentioned previously, localized fault-related pre-impact differential rotation of strata has been suggested by Albat (1988) and Albat and Mayer (1989) to explain problems with the restoration of shatter cone orientations in the western collar of the dome. This may also partly explain the anomalous S3 orientations achieved in the back-rotation in Figs. 5e and 7e. It is possible, however, that these unusual results of back-rotation may be related to the sinuous nature of the pre-impact orientation of the S3 fabric (Lana et al. 2003, Forthcoming), which is a common feature in many high-grade migmatite terranes.

Implications for Impact-Related Deformation in Central Uplifts

Detailed mapping of exposed central uplifts in complex impact craters such as Gosses Bluff, Sierra Madera, and Upheaval Dome (Milton et al. 1996; Wilshire et al. 1972; Kriens et al. 1999) reveals that structures associated with central uplift formation vary as a function of the mechanical properties of the target rock sequence. Thus, in the carbonate-dominated Sierra Madera structure, the central uplift is dominated by steeply-plunging radial folds (Wilshire et al. 1972), while structures like Gosses Bluff, which are underlain by alternating competent and incompetent sedimentary units, display a mosaic pattern of faults and breccia zones separating relatively rigid plates with dimensions of hundreds of meters (Milton et al. 1996). In both cases, the structures reflect the strong tangential shortening that accompanies the initial inward movement of the subcrater basement during central uplift formation (e.g., Kenkmann and Dalwigk 2000; Kenkmann et al. 2000). In many cases, however, the structures may be reactivated or overprinted by slightly younger, predominantly extensional structures associated with the final stages of central uplift formation (Kenkmann et al. 2000; Wieland et al. 2003). In contrast, the internal

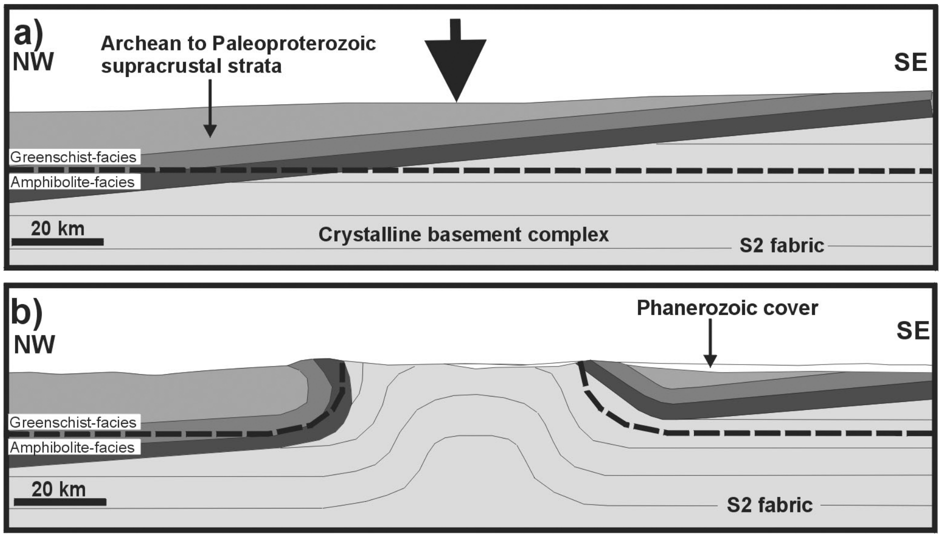

Fig. 8. a) Schematic diagram illustrating S2 in the crystalline basement complex and the horizontal pre-impact metamorphic isograd linked to Bushveld magmatism and NW-tilted core-collar unconformity and supracrustal strata. This obliquity explains the eccentric distribution of the metamorphic isograd relative to the center of the dome in Fig. 1b; b) diagram showing the asymmetric attitude of the collar strata after a uniform 90° rotation and the symmetric geometry of the metamorphic isograd and the S2 fabric.

structure of central uplifts in crystalline targets, such as Puchezh-Katunki, is described as a chaotic "megabreccia" (Ivanov et al. 1996). Ivanov and Deutsch (1998) suggested that these megabreccia blocks form during the shock compression phase of cratering and that acoustic fluidization triggers block oscillation, which, in turn, assists in the hydrodynamic flow necessary to create the central uplift geometry. They propose that large differential rotations can occur in a chaotic manner between adjacent blocks, although the general absence of lithological or structural markers in crystalline rocks makes evaluation of the extent of block rotation difficult.

The Vredefort dome is exceptional among exposed central uplifts not only in its size but also in the extreme depth of erosion. It also comprises both crystalline rocks and a mechanically heterogeneous supracrustal sequence. Recent investigations of the collar structures (Bisschoff 2000; Wieland et al. 2003) confirm that the supracrustal sequence displays both symmetric and asymmetric folds and relatively rigid fault-bounded blocks that display offsets consistent with significant tangential compression. Wieland et al. (2003) have suggested that a major component of this tangential shortening was accommodated in an iris-diaphragm pattern with each segment bounded by transpressive sinistral-reverse faults. This complexity indicates that the simplistic rotations carried out here should not be extended beyond providing first-order approximations of impact-related rotations. More appropriate rotations of smaller segments of the collar about inclined axes could further reduce the scatter of points, although problems are still likely to be encountered with the effects of pre-impact differential rotation of bedding.

The limited exposure of the crystalline basement rocks in the Vredefort dome relative to the collar rocks hampers investigation of large-scale impact-related faulting in the core of the dome; however, we have identified no obvious fault- or breccia-bounded megablocks as previously suggested by Brink et al. (1997). Instead, the continuity of the Archean fabrics suggests that the rotations necessary to create the central uplift were achieved in a more coherent way. One reason for this difference compared with other crystalline central uplifts might be the deep level of erosion of the Vredefort structure. Melosh and Ivanov (1999) have suggested that megablock formation may be inhibited at greater depths because of the increased confining pressure. The absence of megablocks suggests that the necessary displacements and rotations were distributed more evenly through the rock volume in the core of the Vredefort central uplift, allowing less extreme individual rotations and smaller slip-magnitudes. One way in which this could have been done is for the differential rotations and slip to be accommodated along the pervasive pseudotachylitic breccia vein-fracture network. Gibson and Reimold (2003) have argued that the bulk, if not all, of the pseudotachylitic breccias in the Vredefort dome formed during the shock compression phase as a consequence of shock melting, with or without a frictional heating component. The presence of a pervasive network of fractures, locally lubricated by these melts, may have provided the necessary temporary strength degradation in the basement and collar rocks during crater modification to allow a large-scale ductile response and to accommodate the differential rotation and slip required for central uplift formation. Although no evidence exists of large slip-magnitudes along major veins of pseudotachylitic breccia, the consistent mm- to cm-scale displacements of the basement fabrics and collar bedding along the veins (Gibson et al. 1997) suggest that the high-strain deformation could have been distributed as discrete shear in the pseudotachylitic breccia vein-fracture network.

A further influence on the strain behavior of the rocks during central uplift formation is their post-shock temperature. While the rocks in the outer parts of the dome record post-shock temperatures of ~300°C increasing to ~500°C in the inner collar, those in the central core record temperatures in excess of 700°C and locally as high as 1000°C, which is primarily due to the effects of shock heating and uplift of deep crustal levels (Gibson et al. 1998, 2002; Gibson 2002). The presence of anatectic melts, in addition to shock melts, in the central parts of the dome (Gibson 2002; Gibson et al. 2002) may have further assisted strength degradation, however, no obvious small-scale constrictional structures related to the formation of the central uplift have been found in the central parts of the core. This may, in part, reflect the poor exposure but is also likely to reflect the substantial recrystallization and annealing that occurred during cooling from these high temperatures to produce the distinctive granofels in the center of the dome (Fig. 1; Stepto 1990; Gibson et al. 2002).

CONCLUSIONS

Mapping of the Archean structural fabrics within the crystalline basement core of the Vredefort dome has established that the amount of rotation related to formation of the central uplift decreases toward the center of the structure and that the minimum amount of structural uplift was <25 km. The present asymmetry of dips in the collar of the dome can be largely reconciled with symmetric rotation of an inclined NW-dipping target sequence. Complications in this geometry may reflect pre-impact tectonic structures and rotations or complexities associated with central uplift formation and, particularly, the tangential shortening inherent in this process. The absence of clear megablocks and the smooth variation in the orientation of fabrics in the crystalline core of the dome may reflect distributed shear on the shock-induced pseudotachylitic breccia vein-fracture network as well as impact-induced thermal softening.

Acknowledgments–Funding for this project was provided from the Research Council of the University of the Witwatersrand (to W. U. Reimold and R. L. Gibson). The paper benefited from constructive reviews by Thomas Kenkmann and Boris Ivanov. The authors would also like to thank Alex Deutsch for providing information about Russian impact structures. C. Simpson is thanked for her permission to use structural data from an unpublished map in Fig. 4a. University of the Witwatersrand Impact Cratering Research Group Contribution No. 50.

Editorial Handling—Dr. Richard Grieve

REFERENCES

Albat H. M. 1988. Shatter cone/bedding inter-relationship in the Vredefort structure: Evidence for meteorite impact? *South African Journal of Geology* 91:106–113.

Albat H. M. and Mayer J. J. 1989. Megascopic planar shock fractures in the Vredefort structure: A potential time marker? *Tectonophysics* 162:265–276.

Antoine L. A. G., Nicolaysen L. O., and Niccol S. L. 1990. Processed and enhanced gravity and magnetic images over the Vredefort structure and their interpretation. *Tectonophysics* 171:63–74.

Armstrong R. A., Compston W., Retief E. A., Williams L. S., and Welke H. J. 1991. Zircon ion microprobe studies bearing on the age and evolution of the Witwatersrand basin. *Precambrian Research* 53:243–266.

Bisschoff A. A. 1973. The petrology of some mafic and peralkaline intrusions in the Vredefort dome, South Africa. *Transactions of the Geological Society of South Africa* 76:27–52.

Bisschoff A. A. 1982. Thermal metamorphism in the Vredefort dome. *Transactions of the Geological Society of South Africa* 85:43–57.

Bisschoff A. A. 2000. *The geology of the Vredefort dome (Explanation of Geological Sheets 2627CA, CB, CC, CD, DA, DC, and 2727 AA, AB, BA, 1:50000 scale).* Pretoria: Council for Geoscience. 49 p.

Brink M. C., Waanders F. B., and Bisschoff A. A. 1997. Vredefort: A model for the anatomy of an astrobleme. *Tectonophysics* 270:83–114.

Colliston W. P. and Reimold W. U. 1990. *Structural studies in the Vredefort dome; Preliminary interpretations of results on the southern portion of the structure.* Economic Geology Research Unit, Information Circular 229. Johannesberg: University of Witwatersrand. 31 p.

Colliston W. P., Praekelt H. E., and Van der Merwe R. 1999. Recognition of Vredefort-related and pre-Vredefort deformation in the Vredefort impact structure, South Africa (abstract). *Meteoritics & Planetary Science* 34:A27.

French B. M. 1998. *Traces of catastrophe: A handbook of shock-metamorphic effects in terrestrial meteorite impact structures.* LPI Contribution 954. Houston: Lunar and Planetary Institute. 120 p.

Friese A. E. W., Charlesworth E. G., and McCarthy T. S. 1995. *Tectonic processes within the Kaapvaal Craton during the Kibaran (Grenville) orogeny: Structural, geophysical, and isotopic constraints from the Witwatersrand basin and environs.* Economic Geology Research Unit, Information Circicular 292. Johannesburg: University of Witwatersrand. 67 p.

Gibson R. L. 2002. Impact-induced melting in Archaean granulites in the Vredefort dome, South Africa. I.: Anatexis of metapelitic granulites. *Journal of Metamorphic Geology* 20:57–70.

Gibson R. L. and Wallmach T. 1995. Low pressure-high temperature metamorphism in the Vredefort dome, South Africa: Anticlockwise pressure-temperature path followed by rapid decompression. *Geological Journal* 30:319–331.

Gibson R. L. and Reimold W. U. 2001. *The Vredefort impact structure, South Africa (The scientific evidence and a two-day excursion guide).* Council for Geoscience Memoir 92. Pretoria: Council for Geoscience. 111 p.

Gibson R. L. and Reimold W. U. 2003. Thermal and dynamic consequences of impact—Lessons from large impact structures. In *Impact cratering: Bridging the gap between modeling and observations.* LPI Contribution. Houston: Lunar and Planetary Institute. pp. 22–23.

Gibson R. L., Reimold W. U., and Wallmach T. 1997. Origin of pseudotachylites in the Lower Witwatersrand Supergroup, Vredefort dome, South Africa: Constraints from metamorphic studies. *Tectonophysics* 283:241–262.

Gibson R. L., Reimold W. U., and Stevens G. 1998. Thermal metamorphic signature of an impact event in the Vredefort dome, South Africa. *Geology* 26:787–790.

Gibson R. L., Reimold W. U., Phillips D., and Layer P. W. 2000. $^{40}Ar/^{39}Ar$ constraints on the age of metamorphism in the Witwatersrand Supergroup, Vredefort dome (South Africa). *South African Journal of Geology* 103:157–190.

Gibson R. L., Reimold W. U., Ashley A. J., and Koeberl C. 2002. Metamorphism on the moon: A terrestrial analogue in the Vredefort dome, South Africa. *Geology* 30:475–478.

Grieve R. A. F. 1987. Terrestrial impact structures. *Annual Review of Earth and Planetary Science* 15:245–270.

Grieve R. A. F. and Pilkington M. 1996. The signature of terrestrial impacts. *AGSO Journal of Australian Geology and Geophysics* 16:339–420.

Grieve R. A. F. and Therriault A. 2000. Vredefort, Sudbury, Chicxulub: Three of a kind? *Annual Review of Earth and Planetary Science* 28:305–338.

Grieve R. A. F., Robertson P. B., and Dence M. 1981. Constraints on the formation of ring impact structures, based on terrestrial data. In *Mult-ring basins: Formation and evolution.* Proceedings, 12th Lunar and Planetary Science Conference, edited by Schultz P. H. and Merrill R. B. New York: Pergamon, pp. 791-814.

Hart R. J., Welke H. J., and Nicolaysen L. O. 1981. Geochronology of the deep profile through the Archaean basement of Vredefort, with implications for early crustal evolution. *Journal of Geophysical Research* 86:10663–10680.

Hart R. J., Moser D., and Andreoli M. 1999. Archean age for the granulite facies metamorphism near the center of the Vredefort structure, South Africa. *Geology* 27:1091–1094.

Hart R. J., Andreoli M. A. G., Tredoux M., and DeWit M. J. 1990a. Geochemistry across an exposed section of Archaean crust at Vredefort, South Africa: With implications for mid-crustal discontinuities. *Chemical Geology* 82:21–50.

Hart R. J., Andreoli M. A. G., Smith C. B., Otter M. L., and Durrheim R. 1990b. Ultramafic rocks in the centre of the Vredefort structure: Possible exposure of the upper mantle. *Chemical Geology* 82:233–248.

Henkel H. and Reimold W. U. 1998. Integrated geophysical modeling of a giant, complex impact structure: Anatomy of the Vredefort structure, South Africa. *Tectonophysics* 287:1–20.

Ivanov B. A. and Deutsch A. 1999. Sudbury impact event: Cratering mechanics and thermal history. In *Large meteorite imapcts and Planetary evolution II,* edited by Dressler B. O. and Sharpton V. L. Special Paper 339. Boulder: Geological Society of America. pp. 389–397.

Ivanov B. A. and Artemieva N. A. 2002. Numerical modeling of the formation of large impact craters. In *Catastrophic events and mass extinctions: Impacts and beyond,* edited by Koeberl C. and MacLeod K. Special Paper 356. Boulder: Geological Society of America. pp. 619–630.

Ivanov B. A., Kocharyan G. G., Kostuchenko V. N., Kirjakov A. F., and Pevzner L. A. 1996. Puchezh-Katunki impact crater; Preliminary data on recovered core block structure (abstract). 27th Lunar and Planetary Science Conference. pp. 589–590.

Kamo S. L., Reimold W. U., Krogh T. E., and Colliston W. P. 1996. A 2.023 Ga age for the Vredefort impact event and a first report of shock metamorphosed zircons in pseudotachylite breccias and Granophyre. *Earth and Planetary Science Letters* 144:369–388.

Kenkmann T. and von Dalwigk I. 2000. Radial transpression ridges: A new structural feature of complex impact craters. *Meteoritics & Planetary Science* 35:1189–1201.

Kenkmann T., Ivanov B. A., and Stoffler D. 2000. Identification of ancient impact structures: Low-angle faults and related geological features of crater basements. In *Lecture notes in earth sciences 91: Impacts and the early Earth,* edited by Gilmour I. and Koeberl C. Berlin: Springer-Verlag. pp. 279–307.

Killick A. M. 1993. Pseudotachylites of the West Rand Goldfield, Witwatersrand basin, South Africa. Ph.D. thesis (unpublished), Rand Afrikaans University, Johannesburg, South Africa. 273 p.

Koeberl C., Reimold W. U., and Shirey S. B. 1996. Re-Os isotope study of the Vredefort granophyre: Clues to the origin of the Vredefort structure, South Africa. *Geology* 24:913–916.

Kriens K. E., Herkenhoff K. E., and Shoemaker E. M. 1999. Geology of the Upheaval dome impact structure, southeast Utah. *Journal of Geophysical Research* 104:18867–18887.

Lana C., Gibson R. L., Kisters A., and Reimold W. U. 2001. Structural analysis of the core of the central uplift of the Vredefort impact structure, South Africa (abstract #1032). 32th Lunar and Planetary Science. CD-ROM.

Lana C., Gibson R. L., and Reimold W. U. 2002. Archaean crustal evolution of the central parts of the Kaapvaal craton: Evidence from the Vredefort dome, South Africa (abstract #1545). Windhoek, Biannual Congress of the Geological Society of South Africa. CD-ROM.

Lana C., Gibson .R. L., Kisters A., and Reimold W. U. 2003. Archean crustal structure of the Kaapvaal Craton, South Africa—Evidence from the Vredefort dome. *Earth and Planetary Science Letters* 206:133–144.

Lana C., Reimold W. U., Gibson R. L., and Koeberl C. Forthcoming. Nature of the Archean mid-crust in the central parts of the Kaapvaal craton: Evidence from the Vredefort dome, S.A. *Geochimica et Cosmochimica Acta*.

Martini J. E. J. 1991. The nature, distribution, and genesis of the coesite and stishovite associated with the pseudotachylite of the Vredefort dome, South Africa. *Earth Planetary Science Letters* 103:285–300.

McCarthy T. S., Charlesworth E. G., and Stanistreet I. G. 1986. Post-Transvaal structural features of the northern portion of the Witwatersrand basin. *Transactions of the Geological Society of South Africa* 89:311–324.

McCarthy T. S., Stanistreet I. G., and Robb L. J. 1990. Geological studies related to the origin of the Witwatersrand basin and its mineralization—An introduction and a strategy for research and exploration. *South African Journal of Geology* 93:1–4.

Melosh H. J. 1979. Acoustic fluidization: A new geological process? *Journal of Geophysical Research* 84:7513–7520.

Melosh H. J. 1989. *Impact cratering: A geological process.* New York: Oxford University Press. 245 p.

Melosh H. J. and Ivanov B. A. 1999. Impact crater collapse. *Annual Review of Earth and Planetary Science* 27:385–415.

Milton D. J., Glikson A. Y., and Brett R. 1996 Gosses Bluff—A latest Jurassic impact structure, central Australia. Part 1: Geological structure, stratigraphy, and origin. *AGSO Journal of Australian Geology and Geophysics* 16:453–486.

Minnitt R. C. A., Reimold W. U., and Colliston W. P. 1994. *The geology of the Greenlands Greenstone Complex and selected granitoid terranes in the south-eastern quadrant of the Vredefort dome.* Economic Geology Research Unit, Information Circular 28. Johannesburg: University of Witwatersrand. 35 p.

Moser D. E., Flowers R. M., and Hart R. J. 2001. Birth of the Kaapvaal Tectosphere 3.08 billion years ago. *Science* 291:465–468.

Reimold W. U. and Colliston W. P. 1994. Pseudotachylites of the Vredefort dome and the surrounding Witwatersrand basin, South Africa. In *Large meteorite impacts and planetary evolution,* edited by Dressler B. O., Grieve R. A. F., and Sharpton V. L. Special Paper 293. Boulder: Geological Society of America. pp. 177–196.

Reimold W. U., Colliston W. P., and Wallmach T. 1992. Comment on

"Nature, provenance, and distribution of coesite and stishovite in the Vredefort structure" by J. E. J. Martini. *Earth and Planetary Science Letters* 12:213–217.

Roering C., Barton J. M., Jr., and Winter H. de la R. 1990. The Vredefort structure: A perspective with regard to new tectonic data from adjoining terranes. *Tectonophysics* 171:7–22.

Schultz P. H. 1997. Assessing impact trajectory in the geologic record Sudbury impact event: Cratering mechanics and thermal history (abstract #6106). Large Meteorite Impacts II and Planetary Evolution. CD-ROM.

Slawson W. F. 1976. Vredefort core: A cross-section of the upper crust? *Geochimica et Cosmochimica Acta* 40:117–121.

Spray J. G. 1997. Superfaults. *Geology* 25:579–582.

Spray J. G., Kelley S. P., and Reimold W. U. 1995. Laser-probe ^{40}Ar-^{39}Ar dating of pseudotachylites and the age of the Vredefort impact event. *Meteoritics & Planetary Science* 30:335–343.

Stepto D. 1979. A geological and geophysical study of the central portion of the Vredefort dome structure. Ph.D. thesis (unpublished), University of Witwatersrand, Johannesburg, South Africa. 453 p.

Stepto D. 1990. The geology and gravity field in the central core of the Vredefort structure. *Tectonophysics* 171:75–103.

Stevens G., Gibson R. L., and Droop G. T. R. 1997. Mid-crustal granulite facies metamorphism in the Central Kaapvaal craton: The Bushveld Complex connection. *Precambrian Research* 82: 113–132.

Tredoux M., Hart R. J., Carlson R. W., and Shirley S. B. 1999. Ultramafic rocks at the center of the Vredefort structure: Further evidence for the crust on edge model. *Geology* 27:923–926.

Trieloff M., Reimold W. U., Kunz J., Boer R. H., and Jessberger E. K. 1994. ^{40}Ar-^{39}Ar thermochronology of pseudotachylites at the Ventersdorp Contact Reef, Witwatersrand basin. *South African Journal of Geology* 97:365–384.

Turtle E. P. and Pierazzo E. 1998. Constraints on the size of the Vredefort impact crater from numerical modeling. *Meteoritics & Planetary Science* 33:483–490.

Wieland F., Gibson R. L., Reimold W. U., and Lana C. 2003. Structural evolution of the central uplift of the Vredefort impact structure, South Africa (abstract). *Meteoritics & Planetary Science* 38:A21.

Wilshire H. G., Offield T. W., Howard K. A., and Cummings D. 1972. Geology of the Sierra Madera cryptoexplosion structure, Texas. United States Geological Survey, Professional Paper 599-H. 42 p.